무중력에서의 비예혼합 메탄-공기 화염의 전산
II. 화염의 반경과 두께

박 외 철
부경대학교 안전공학과
(2004. 4. 14. 접수 / 2004. 8. 19. 채택)

Computation of Nonpremixed Methane-Air Flames in Microgravity
II. Radius and Thickness of Flame

Woe-Chul Park
Department of Safety Engineering, Pukyong National University
(Received April 14, 2004 / Accepted August 19, 2004)

Abstract : To evaluate the numerical method in simulation of diffusion flames and to see the effects of strain rate and fuel concentration on the flame radius and thickness, the nonpremixed methane-air counterflow flames in microgravity were simulated axisymmetrically by using the NIST Fire Dynamics Simulator (FDS). The 1000°C based flame radius and thickness were investigated for the mole fraction of methane in the fuel stream, x_m = 20, 50, and 80%, and the global strain rates a_g = 20, 60, and 90s^{-1} for each mole fraction. The flame radius increased with the global strain rate while the flame thickness decreased linearly as the global strain rate increased. The flame radius decreased as the mole fraction increased, but it was not so sensitive to the mole fraction compared with the global strain rate. Since there was good agreement in the nondimensional flame thickness obtained with OPPDIF and FDS respectively, it was confirmed that FDS is capable of predicting well the counterflow flames in a wide range of strain rate and fuel concentration.

초 록 : 확산화염 시뮬레이션에 대해 수치법을 검증하고 변형률과 연료농도가 화염반경과 두께의 변화에 미치는 영향을 조사하기 위해, Fire Dynamics Simulator (FDS)를 사용하여 무중력의 비예혼합 메탄-공기 대향류 화염을 축대칭으로 모사하였다. 연료 중 메탄의 몰분율 x_m = 20, 50, 80%와 각각의 몰분율에서 세가지 변형률 a_g = 20, 60, 90s^{-1}의 1000°C 기준 화염반경과 화염두께를 조사하였다. 변형률이 클수록 화염반경은 증가하였으나 화염두께는 거의 선형적으로 감소하였다. 또 화염반경은 메탄농도가 높을수록 감소하였으나, 변형률의 영향만큼 메탄농도에 민감하지 않았다. FDS와 OPPDIF로 각각 구한 무차원 화염두께가 잘 일치하므로, 넓은 범위의 연료농도와 변형률에서 FDS가 대향류 확산화염의 화염구조를 잘 예측할 수 있음을 확인하였다.
Key Words : counterflow flame, microgravity, global strain rate, fuel concentration, flame thickness, flame radius

Nomenclature

a_g : global strain rate
D : inside diameter of ducts, 15mm
L : separation distance between two ducts, 15mm
x_m : mole fraction of methane in fuel stream
r_f : flame radius based on 1000°C
t : duct thickness, 0.5mm
t_f : flame thickness based on 1000°C
τ : nondimensional flame thickness(= t_f/L)
ρ : nondimensional flame radius (= r_f/D)

1. Introduction

In the Part I[1], the methane-air nonpremixed counterflow flames in microgravity were simulated by using the NIST Fire Dynamics Simulator (FDS)[2]. The results showed an accurate prediction of temperature and axial

wcpark@pknu.ac.kr

velocity profiles in a wide range of fuel concentrations and global strain rates. There was good agreement in the temperature and axial velocity profiles between the axisymmetric (two-dimensional) simulations with FDS and one-dimensional simulations with OPPDIF[3]. The flame thickness, flame positions and stagnation points were also accurately predicted. In addition to comparisons of the temperature and axial velocity profiles between 1-D and 2-D simulations, comparison of the radius and thickness of the flame for the fuel concentration and global strain rate may be another evaluation for the numerical method.

The objectives of this study are to evaluate the two-dimensional simulations through comparisons of the flame thickness and radius between the one-dimensional and two-dimensional simulations, and to investigate the effects of the global strain rate and fuel concentration on the flame radius and thickness of the counterflow flame in microgravity. Two new nondimensional parameters, the flame thickness τ and the flame radius ρ, both based on T = 1000°C, were introduced in the present study.

2. Methodology

The counterflow burner shown in Fig. 1 is the same that used in the Part I[1]. The fuel gas which is a mixture of methane and nitrogen is supplied through the lower fuel duct, and the air flows in the oxidizer duct. D is the inside diameter of ducts, t is the duct thickness, and L is the separation distance between the two ducts. Combustion takes place in quiescent nitrogen gas.

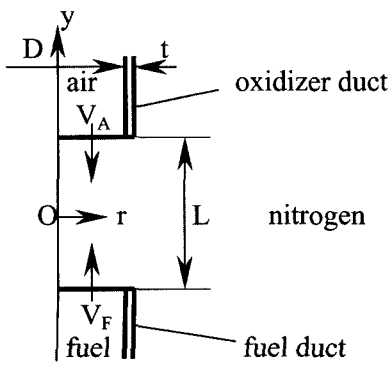

Fig. 1. Schematic of the counterflow burner

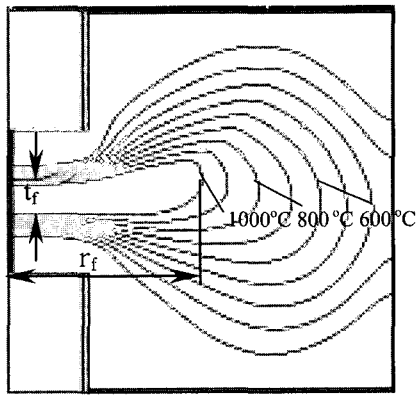

(a) Flame radius and thickness measured from isotherms (2-D)

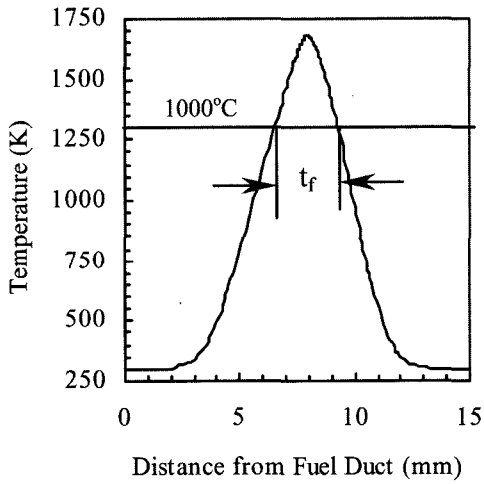

(b) Flame thickness measured from temperature profile (1-D)

Fig. 2. Measurement of flame radius and thickness

The radius and thickness of the flame were measured from the isotherm of 1000°C as shown in Fig. 2 (a), which was obtained by axisymmetric (2-D) simulation with FDS. On the other hand, since the isotherms are not available in 1-D simulations with OPPDIF, the flame thickness was measured from the temperature profile as depicted in Fig. 2(b). For accuracy, the radius and thickness of the flame were measured by the number of pixels on the monitor from the isotherms and temperature profiles magnified four-times.

The global strain rate ag is defined as $a_g = -2V_A[1-(\rho_F/\rho_A)^{0.5} V_F/V_A]/L$. Here V is the velocity at the duct exits, ρ is the density at 1 atm, 25°C, and the subscripts A represents the air and F does the fuel. V_A, the average velocity in the oxidizer duct, and VF, that in the fuel duct, have the same magnitude but opposite

directions, that is, $V_A = -V_F$. The size of the computational domain, 40mm×40mm, and the grid size, 0.5mm in the r- and x-directions, were used. All the numerical procedures are the same as those in the Part I[1]. As numerical parameters, the global strain rate, a_g = 20, 60 and 90 s^{-1} and the methane mole fraction in the fuel stream, x_m = 20, 50 and 80% were taken.

3. Results and Discussion

3.1. x_m = 20%

Three different values of the fuel concentration, that is, the mole fraction of methane in the fuel stream, x_m = 20% which is near extinction, 60%, a moderate fuel concentration, and 80%, a fuel rich concentration, were chosen as numerical parameters to see the effects of the fuel concentration on the flame structures. Fig. 3 shows the isotherms of the flame at a_g= 20, 60 and 90 s^{-1}, respectively, for the fuel of x_m= 20% (20% methane and 80% nitrogen by volume in the fuel stream), obtained by axisymmetric (2-D) simulations. Each isotherm has 100°C increment, and the inner-most one corresponds to 1000°C. Changes in the flame thickness and radius with the global strain rate, i.e., thinner flame thickness and larger flame radius with the increasing strain rate, are clearly shown. Decreasing thickness and increasing radius with the increasing global strain rate is due to the increasing velocity at the duct exits, which increases with the global strain rate as can be seen in the definition of a_g. The flame is more stretched with the axial velocity as the strain rate increases from a_g = 20 to 60 and 90 s^{-1}. Note that the isotherms are not available in the 1-D simulations with OPPDIF[3], where the flame is assumed one-dimensional.

In Fig. 4, the 1000°C based flame radius is compared for a_g = 20, 60 and 90 s^{-1} when x_m = 20%. The flame radius, ρ, was measured from the isotherm of 1000°C, and nondimensionalized by the inside diameter of the two ducts, D. ρ increases with the global strain rate almost linearly. The axial velocity in the fuel and oxidizer streams is proportional to the global strain rate, and this results in flame stretch. Comparison of the flame radii between 1-D and 2-D is not possible since the 1-D simulations provide the flame thickness only.

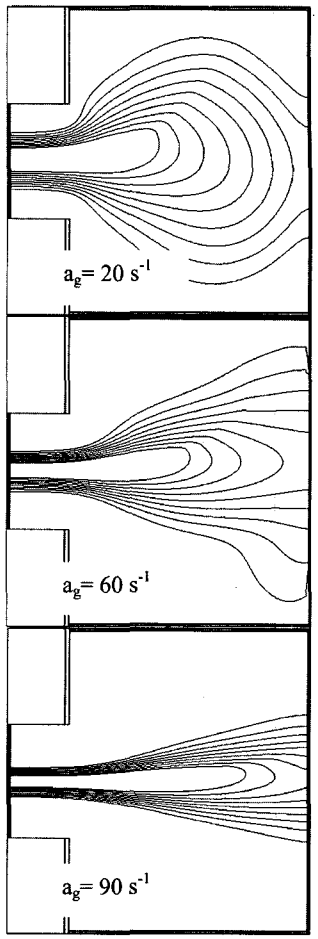

Fig. 3. Isotherms for x_m = 20% (2-D)

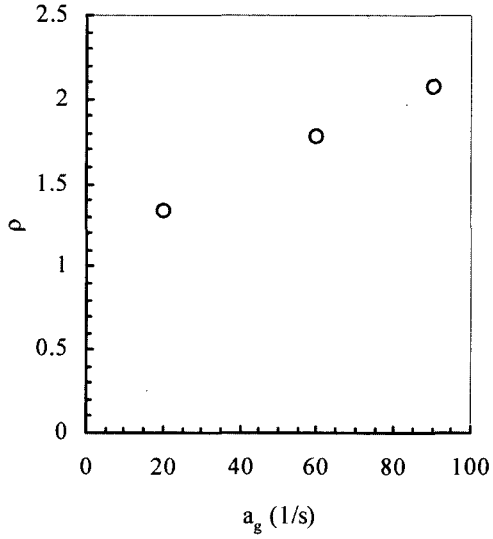

Fig. 4. Flame radius vs. global strain rate for x_m = 20% (2-D)

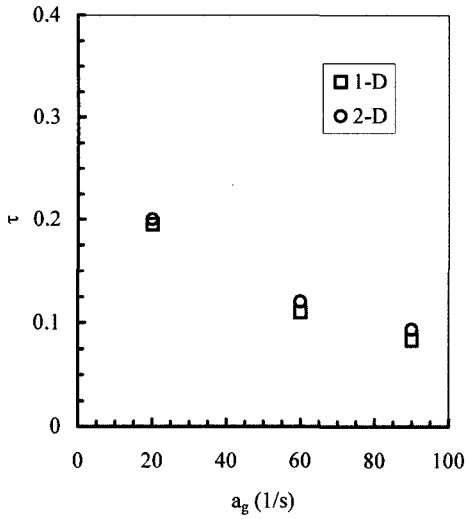

Fig. 5. Flame thickness vs. global strain rate for x_m = 20%.

Meanwhile, the flame thickness at the duct centerline, τ, nondimensionalized by the distance between the two ducts, L, decreases with the increasing global strain rate as shown in Fig. 5. The flame thickness of 2-D simulations is in very good agreement with that of 1-D simulations for all the three values of the global strain rate. It shows that the flame thickness decreases nearly linearly with the increasing global strain rate.

3.2. x_m = 50%

For the moderate fuel concentration, $x_m = 50\%$, which is the mixture of 50% methane (CH_4) and 50% nitrogen by volume in the fuel stream of the fuel duct, Fig. 6 compares the flames represented by isotherms. It is clearly shown that the flame becomes thinner and its radius increases with the global strain rate by stretching the flame with the increasing axial velocity. This is consistent with the results of the fuel concentration $x_m = 20\%$ shown in Fig. 3. The flames of $x_m = 50\%$ are thicker compared with those of $x_m = 20\%$ at all the three global strain rates. The flame thickness thus increases with fuel concentration. The flame radius does not vary much with the fuel concentration whereas the flame thickness does.

Fig. 7 shows quantitatively variation of the flame radius versus the global strain rate for x_m = 50%. Increasing flame radius with the global strain rate is similar to that for x_m = 20%, but is slightly away from the near-linear relation shown in Fig. 4.

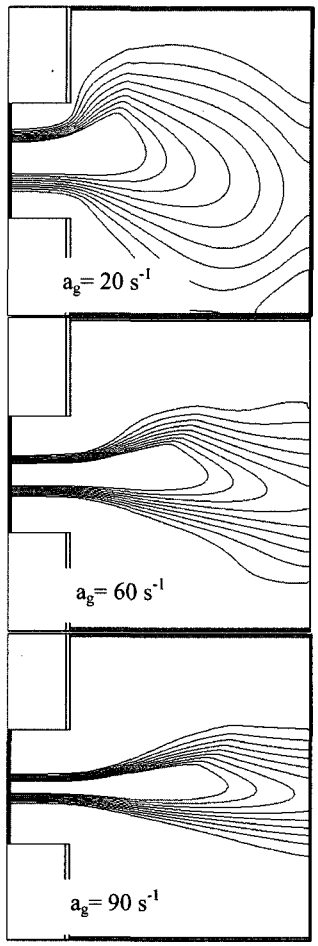

Fig. 6. Isotherms for x_m = 50% (2-D)

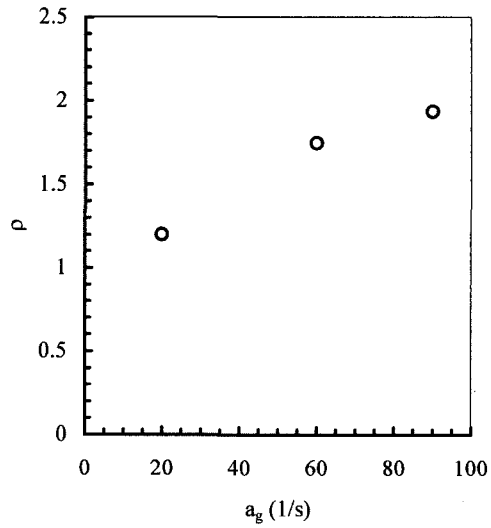

Fig. 7. Flame radius vs. global strain rate for x_m = 50% (2-D)

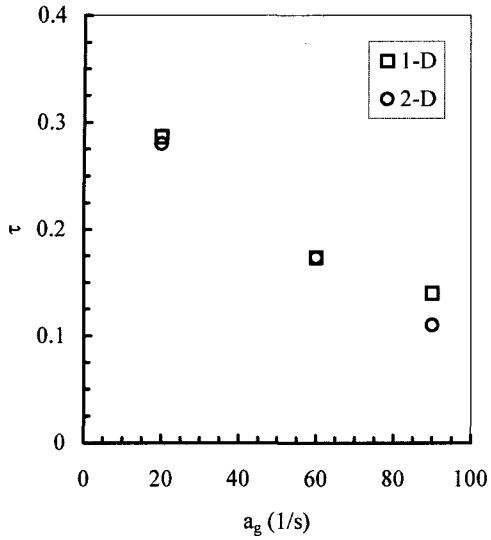

Fig. 8. Flame thickness vs. global strain rate for xm = 50%

On the other hand, In Fig. 8, the flame thickness computed by the 2-D simulations decreases linearly with increasing global strain rate. The flame thickness of the 2-D simulations is almost the same as the 1-D simulations except for a_g = 80 s^{-1}. Compared with the lower fuel concentration of x_m = 20%, the flame radii at the same global strain rate are not much different (see Figs. 4 and 7). Figs. 5 and 8, however, shows that the flame thickness at x_m = 50% is much thicker than that at x_m = 20%, and that the flame thickness increases with the fuel concentration. It is noted that change in the flame thickness is highly sensitive to the fuel concentration when the global strain rate is low. Although the cause of discrepancy in the flame thickness at a_g = 80 s^{-1} is not known, computation of the flame thickness with the 1-D simulations may have large errors at the high global strain rate.

3.3. x_m = 80%

The isotherms of the flame for the fuel rich case, x_m = 80% (80% methane and 10% nitrogen in the fuel stream) are shown in Fig. 9. Changes in the flame shape with the global strain rate are not much different from those of the previous cases, 20%CH_4 + 80%N_2 and 50%CH_4 + 50%N_2.

Variation of the flame radius versus the global strain rate in Fig. 10, measured from the isotherms in

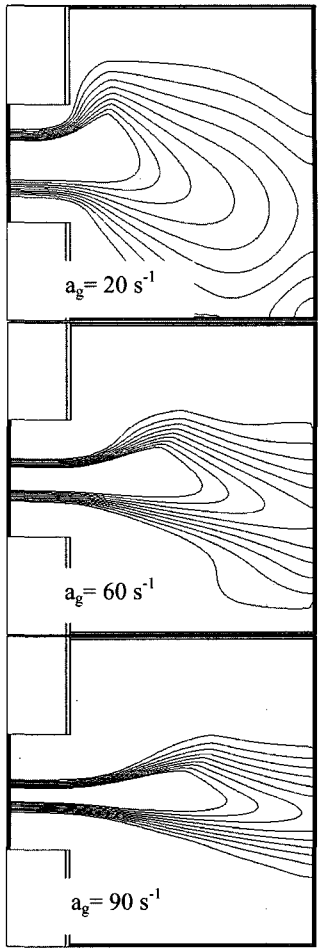

Fig. 9. Isotherms for x_m = 80% (2-D)

Fig. 9 of the 2-D simulations, is similar to that of xm= 50% shown in Fig. 7. Since the flame radius of xm= 50% for a_g = 20, 60 and 90 s^{-1} is almost the same as the corresponding flame radius of x_m = 80%, the influence of the fuel concentration on the flame radius is negligible when the fuel concentration is high.

The flame thickness compared for the three global strain rates in Fig 11 is in good agreement between the 1-D and 2-D simulations. The flame thickness of the high fuel concentration, x_m = 80%, decreases linearly with the increasing global strain rate similarly to the moderate fuel concentration, x_m = 50%. The decreasing rate in the flame thickness with the increasing global strain rate for x_m = 80% is also nearly the same as that for x_m = 80%.

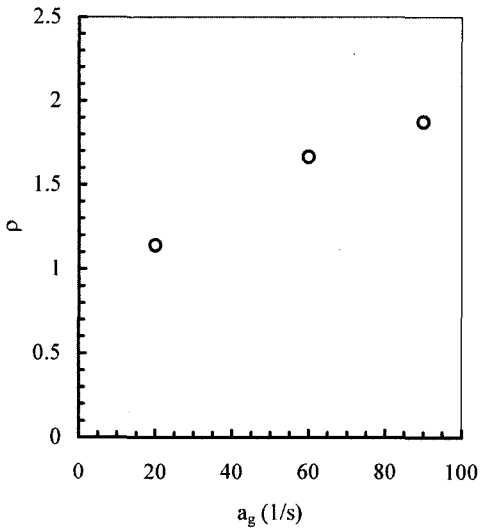

Fig. 10. Flame radius vs. global strain rate for x_m = 20% (2-D)

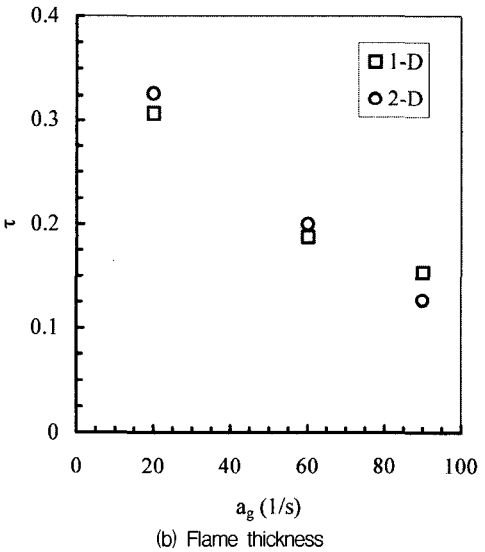

(b) Flame thickness

Fig. 11. Flame thickness vs. global strain rate for fuel of x_m = 80%

4. Conclusions

The nitrogen diluted methane-air counterflow flames in microgravity were simulated by using FDS and OPPDIF, respectively. The 1000°C based radius and thickness of the flames were investigated for the numerical parameters of the mole fraction of methane in the fuel stream, x_m = 20, 50, 80%, and the global strain rate, a_g = 20, 60 and 90 s^{-1}, of each xm. The following conclusions were drawn from the results:

1) The flame thickness was in good agreement between the 1-D and 2-D simulations, and it was confirmed that FDS may be used to the counterflow flame in a wide range of the global strain rate and fuel concentration.

2) The flame thickness decreased linearly with the increasing global strain rate. Its decreasing rate was almost the same for x_m = 50% and 80%.

3) Variation of the flame thickness was highly sensitive to the fuel concentration when the global strain rate was low.

4) The flame radius increased with the global strain rate by stretching the flame, and the influence of the fuel concentration on the flame radius was very small at the moderate and high fuel concentrations.

References

1) W. C. Park, "Computation of Nonpremixed Methane-Air Diffusion Flames in Microgravity, I. Profiles of Flame Temperature and Axial Velocity," J. Korea Inst. Industrial Safety, Vol. 19, No. 1, pp. 124~130, 2004.

2) K. B. McGrattan, H. R. Baum, R. G. Rehm, A. Hamins, G. P. Forney, J. E. Floyd, S. Hostikka and K. Prasad, Fire Dynamics Simulator (Version 3) - Technical Reference Guide, NIST, Gaithersburg, MD, U.S.A., 2003.

3) A. Lutz, R. J. Kee, J. Grcar and F. M. Rupley, "A Fortran Program Computing Opposed Flow Diffusion Flames," SAND96-8243, Sandia National Laboratories, Livermore, CA, U.S.A., 1997.